Supporting Information

Application of a Cytochrome P450 Enzyme eluted from Encapsulated Biomaterials to the Catalysis of Enantioselective Oxidation

*Hiroyuki Nagaoka**

Sanyo Shokuhin Co., Ltd. R & D, 555-4 Asakura, Maebashi, Gunma 371-0811, Japan

E-mail: hnagaoka@sanyofoods.co.jp, Tel: +81-27-220-3471, Fax: +81-27-220-3477

Abbreviations: ME: membrane-bound enzyme, GA: glutaraldehyde, FD: freeze-dried, Has: heme acquisition system, NAD(P): nicotinamide adenine dinucleotide, FAD: flavin adenine dinucleotide, PP-gel: calcium-alginate-gel-containing PP, CLME: cross-linked ME, CMME: a compound-modified ME, AGME: PEG (MW: 1000/4000 = 2/1)-aggregated ME, *S*-**1**: *S*-(+)-1-(6-methoxynaphthalen-2-yl)ethanol, *S*-**2**: *S*-(+)-1-(2-naphthyl) ethanol, HBP: heme-binding protein. PQQ-ADH: pyrroloquinoline quinone alcohol dehydrogenase, Cyt*c*O: cytochrome c oxidase, Cyt-P450: oxygen-driven cytochrome P450 enzyme, P450: cytochrome P450 enzyme.

Table of Contents

1. General procedure for reactions using CMME and AGME

A calibration curve configured, the chromatograms of the *rac*-**1** biotransformation with ME derivatives were shown. Enantiomeric excess (ee) values, chemical yield ratio (% yield)/convertion ratio of all compounds were obtained from chiral HPLC analysis.[1]

1-1. Calibration curve configured using HPLC.

The ee was calculated for either *rac*-**1** (0.8 mM or 1.2 mM) or *rac*-**2** (0.8 mM or 1.2 mM), which were separated with either a Daicel Chiralcel OB-H column ((S)-isomer/(R)-isomer/product ketone = 7.8/8.8/11.6 min) or a Daicel Chiralpak AS-H column ((S)-isomer/(R)-isomer/product ketone = 7.5/8.25/9.5 min) connected to an HPLC LC-10A system (Shimadzu). Analytical conditions were as follows: mobile phase, n-hexane/IPA: 9/1, flow rate: 1.0 mL/min, temperature: 30 °C, wavelength: UV 254 nm. The stereochemistry of the isolated optically active alcohol was identified by comparing the values (+ or –) for the specific rotation detected using a polarimeter, as done previously. [1]

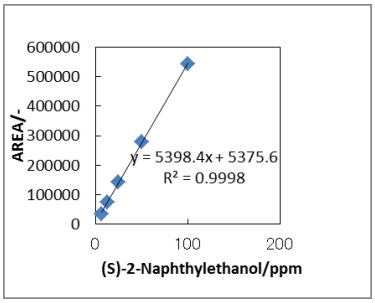

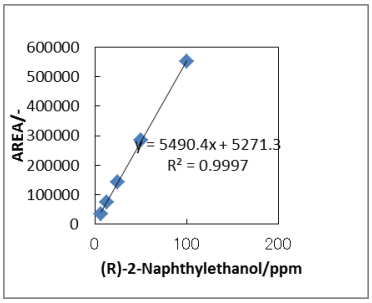

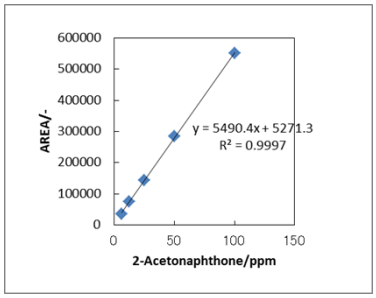

Conc./ppm	(*R*)-2/abs‡	(S)-2/abs‡	ketone/abs†
3.125	18408	18403	-
6.25	34455	34671	64884
12.5	69207	69837	129479
25	133042	134274	256966
50	263249	267577	509690
100	515506	524152	983200

‡Absorbance of HPLC analysis, †Average

1-2. Data of chromatograms

The time course/chromatograms of the asymmetric oxidation of *rac*-**1** (1.2 mM) using a $CLME_a$ (20 mg) was monitored and quantitatively analyzed under the suggested conditions.[1]

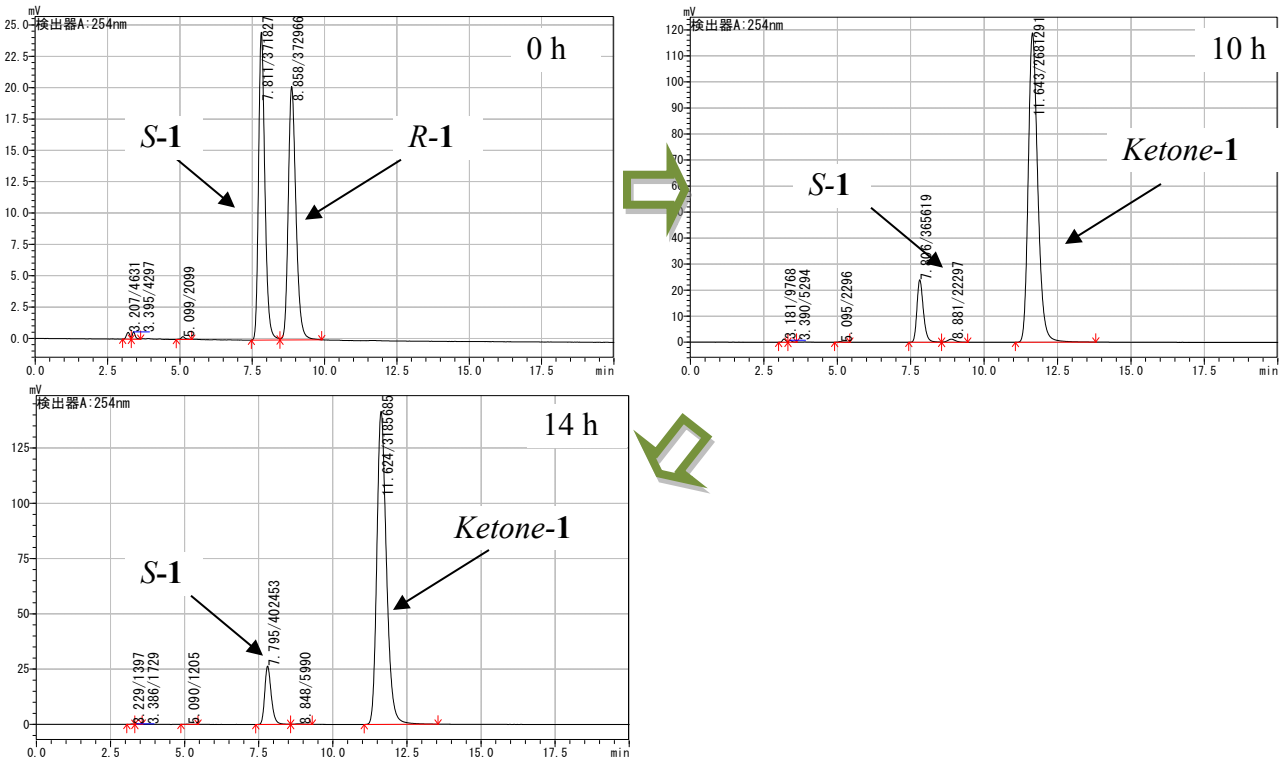

Time/h	*S*-**1**/Abs‡	*R*-**1**/abs‡	Ketone/Abs‡	%ee	Avg† (%ee)
0	384592 371827	386537 372966	- -	0.252 0.152	0.20
10	341321 365619	27703 22297	2437138 2681291	84.985 88.50	86.74
14	421760 402453	2286 1190	3429781 3185685	98.92 99.41	99.17

‡Absorbance of HPLC analysis, †Average

Differences in the activity between ME-fractions separated by centrifugation and the ME-derivatives.

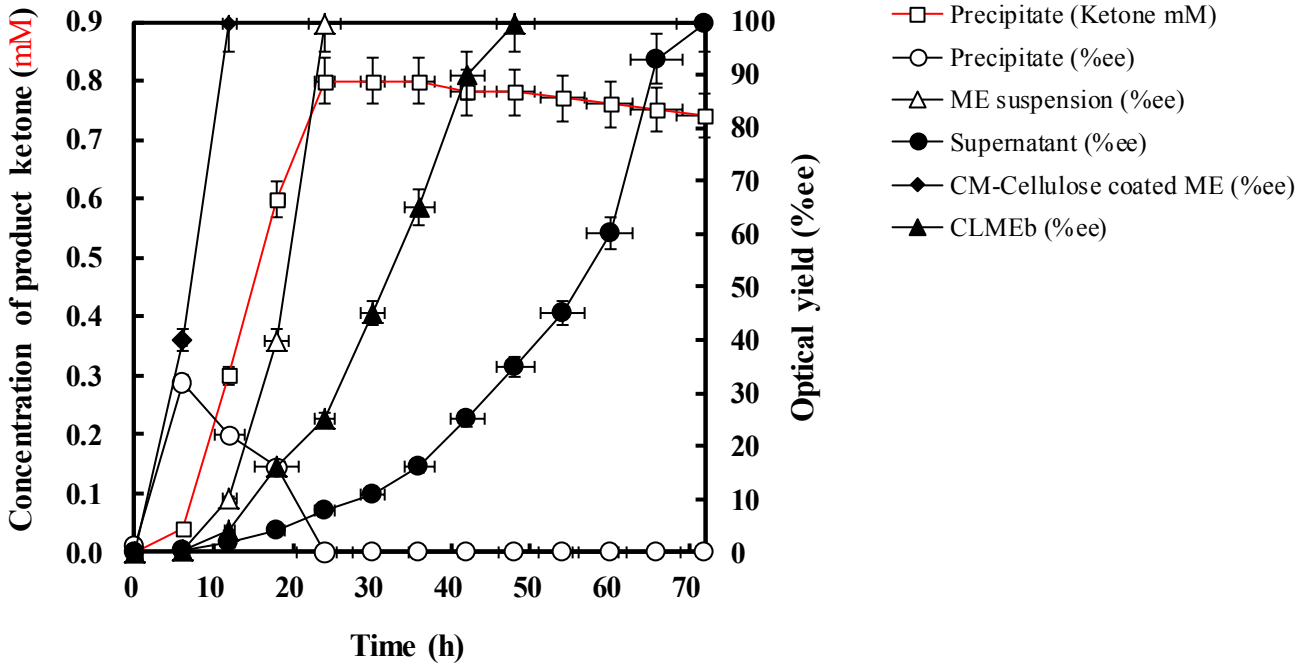

Figure S1. Time course of the asymmetric oxidation activity: (-△-) eluent from the ME-suspension of the PP-gel (5.0 mL), (-●-) supernatant of the ME-suspension acquired via centrifugation (5.0 mL), (-□-: mM, -○-: %ee) aqueous suspension of the sample 1 precipitate acquired via centrifugation (100 mg/5.0 mL D.W.), (-♦-) CM-cellulose-coated ME (20 mg/5.0 mL D.W.), and (-▲-) cross-linked ME_b ($CLME_b$) treated with 30% (w/v) aqueous $(NH_4)_2SO_4$) (20 mg/5.0 mL 50 mM glycine–NaOH (pH 9.0)). A substrate solution (*rac*-**1**: 20 μL, 20,000 ppm) was then poured into a test tube (18 mm × 15 mL) containing each of the samples prepared above.

As shown in Figure 1, while the activity of the ME suspension shows a 24 h biotransformation time, the highest asymmetric oxidation activity was observed in the CMC-ME reaction (13 h), and the lowest activities were observed for the $CLME_b$ reaction (48 h) and ME supernatant reaction (72 h). The ME-suspension, supernatant, precipitate, and CMC-ME may function in the presence of O_2 via a reactive oxygen species ($Fe^{2+} + O_2 \rightarrow Fe^{3+}–O–O^- \rightarrow Fe^{4+}=O$ (+ *rac*-**1**) $\rightarrow Fe^{2+} + H_2O$).[3c] This suggests that the iron electron-transfer system may lie in the hydrogen peroxide-driven $P450_{BS\beta}$ —an HBP that depends on oxygen instead of a redox cofactor (e.g., NAD(P)H).[3]

2. Data of FTIR/ICP-ACS/IC analysis for the no necessity of $(NH_4)_2SO_4$ process.

To investigate the reason relevant for the poor activity of $CLME_b$, the residue content (%) of raw materials (i.e., $(NH_4)_2SO_4$ and sodium alginate) per CMME was examined. To investigate functional group of 1) PP, 2) sodium alginate, 3) PEG (4000), 4) SC1 (PEG (4000)-ME (1) not treated with $(NH_4)_2SO_4$), 5) SC2 (PEG (4000)-ME (2) treated by the precipitation process using 30% (w/v) aqueous $(NH_4)_2SO_4$), and 6) SC3 ($CLME_b$ treated by $(NH_4)_2SO_4$), these samples were analyzed using a portable ATR instrument (A2 Technologies; ML version).

2-1. ML FTIR instrument analysis

A single bounce internal reflection method using a diamond crystal was applied to acquire spectra of the PP, PEG (4000)-MEs (SC1 and SC2), $CLME_b$, and sodium alginate. The samples were placed on the diamond crystal to acquire their spectra.

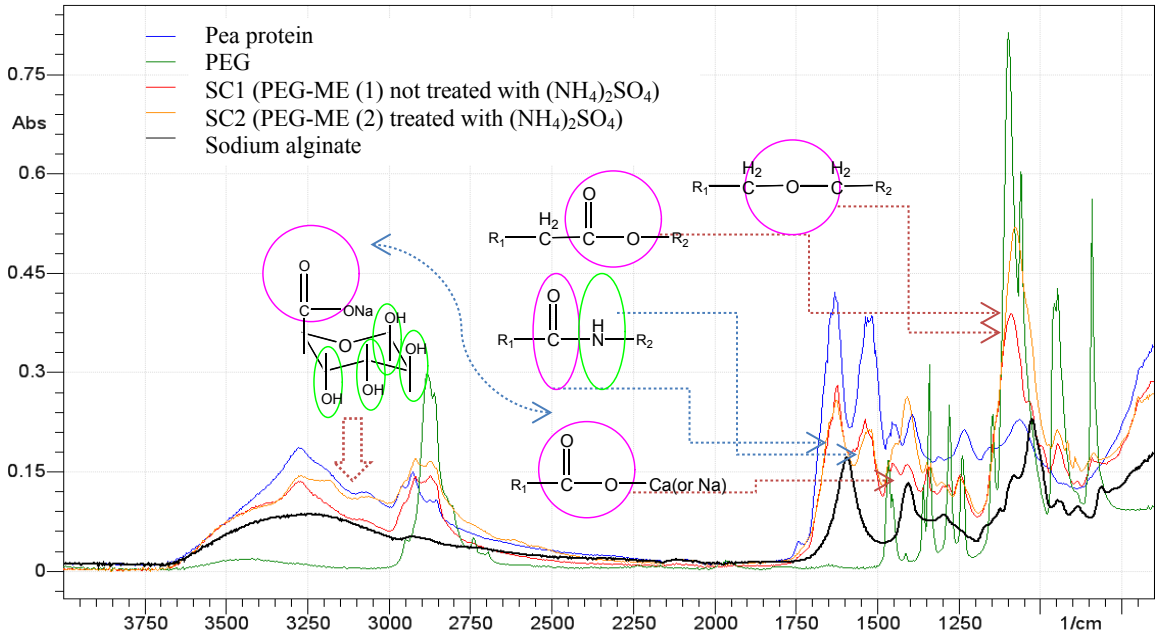

Figure S2. Differences in the content of functional groups among four samples: (1) SC1 (PEG (4000)-ME (1) not treated with $(NH_4)_2SO_4$), (2) SC2 (PEG (4000)-ME (2) treated with 30% (w/v) aqueous $(NH_4)_2SO_4$), (3) pea protein (PP), and (4) sodium alginate.

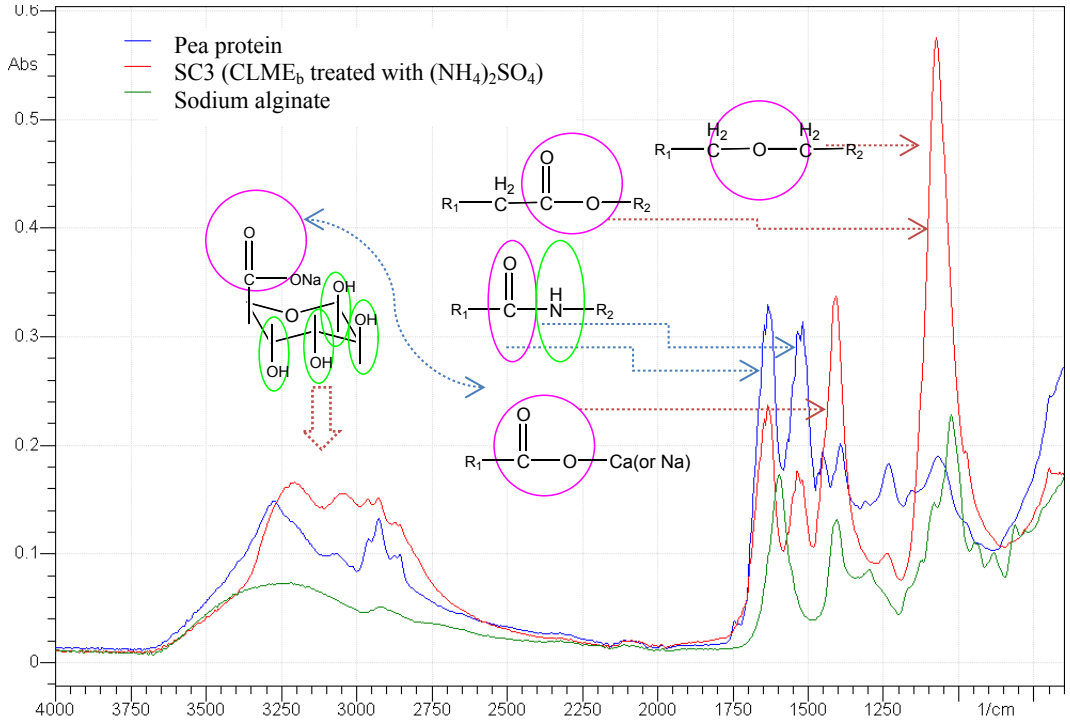

Figure S3. Difference in the content of functional groups among three samples: (1) $CLME_b$ (SC3: cross-linked ME treated with 30% (w/v) aqueous $(NH_4)_2SO_4$), (2) pea protein (PP), and (3) sodium alginate. *To ensure uniform contact, each sample was pressed to a crystal by a pressure device that was attached to the ML FTIR instrument. SC1 shows the PEG (4000)-MEs (1) treated without the saturated $(NH_4)_2SO_4$; whereas SC2 and SC3 show the PEG-MEs (2) and cross-linked MEs, respectively, treated with the 30 (v/v%) saturated $(NH_4)_2SO_4$ process.

Table S1. Content of elements: improvement of the purification processes of raw materials residue content for MEs treated or not treated with $(NH_4)_2SO_4$ from elements identified in **Figures S1 and S2**.

Sample	**FTIR analysis**			
	950–1250 cm^{-1} i.e., sulfate	**1250–1500 cm^{-1}** i.e., calcium alginate	**1500–1750 cm^{-1}** i.e., Pea Protein	**Residues**
PP	0.19 abs	0.24 abs	0.4 abs	—
SC3: $CLME_b$[a]	0.58 abs	0.32 abs	0.24 abs	$(NH_4)_2SO_4$ Calcium-Alginate
SC1: PEG (4000)-ME[b]	0.42 abs	0.17 abs	0.3 abs	—
SC2: PEG (4000)-ME[c]	0.58 abs	0.28 abs	0.3 abs	$(NH_4)_2SO_4$ Calcium-Alginate

[a]$CLME_b$ includes the process of "$(NH_4)_2SO_4$" precipitation.

[b]PEG (4000)-ME (SC1) does not includes the process of "$(NH_4)_2SO_4$" precipitation but centrifugation.
[c]PEG (4000)-ME (SC2) includes the process of "$(NH_4)_2SO_4$" for precipitation.
[d]highest wt% (red) shows the reminder of "$(NH_4)_2SO_4$" in the precipitation process.
[e]lowest wt% (blue) shows no reminder but a higher oxygen (O_2) is detected to PP.

2-2. Result of the section 2-1

The FTIR spectra showed a significant difference between the ME not treated with $(NH_4)_2SO_4$ (i.e., SC1) and ME treated with $(NH_4)_2SO_4$ (i.e., SC2 and SC3). As shown in **Figures S2 and S3**, when SC1 is compared with SC2 and SC3 ($CLME_b$), it can be seen that both sodium alginate (range, 1250–1500 cm^{-1}) and $(NH_4)_2SO_4$ (range, 950–1250 cm^{-1}) were dramatically reduced in the untreated catalyst. This result indicated that when preparing SC1, not treated with $(NH_4)_2SO_4$, the raw materials (i.e., sodium alginate and $(NH_4)_2SO_4$) can be removed successfully. This means the ME-redox protein incorporating an iron electron-transfer system may be effectively concentrated, reducing the activity of $CLME_b$ (i.e., direct evidence) (see **Table S1**). Furthermore, to explain why SC1 has a spectrum apparently showing a sulfate (SO),[3c] it was speculated that oxygen absorption in the PP gel is processed under aeration, and then an oxygen-driven cytochrome P450 enzyme (Cyt-P450, a HBP) is formed/eluted, which leads to the formation of a reactive oxygen species via an iron electron-transfer system (Cyt-P450[3a-3c]: cysteine– Fe^{2+} + O_2 → Fe^{3+}–O–O^- → Fe^{4+}=O (oxidizing *rac*-**1**) → Fe^{2+} + H_2O), resulting in water solubility (PP → ME), leading to the appearance of sulfate (SO: a superoxoiron–cysteinate) in the range 950–1250 cm^{-1}.[3]

2-3. ICP-AES analysis and IC analysis in between PP and ME derivatives

In the measurements of metal contents of between PP, $CLME_b$ (before FD and after FD), and PEG(4000)-ME (1: without $(NH_4)_2SO_4$ process and 2: with $(NH_4)_2SO_4$ process), the each samples (0.5 g) was added to a 100 mL beaker with purified water (50 mL) and 60%-HNO_3 (Kokusan, 10 ml), and then digested by heating on a hotplate about 1 h: the ICP-AES analysis was done.

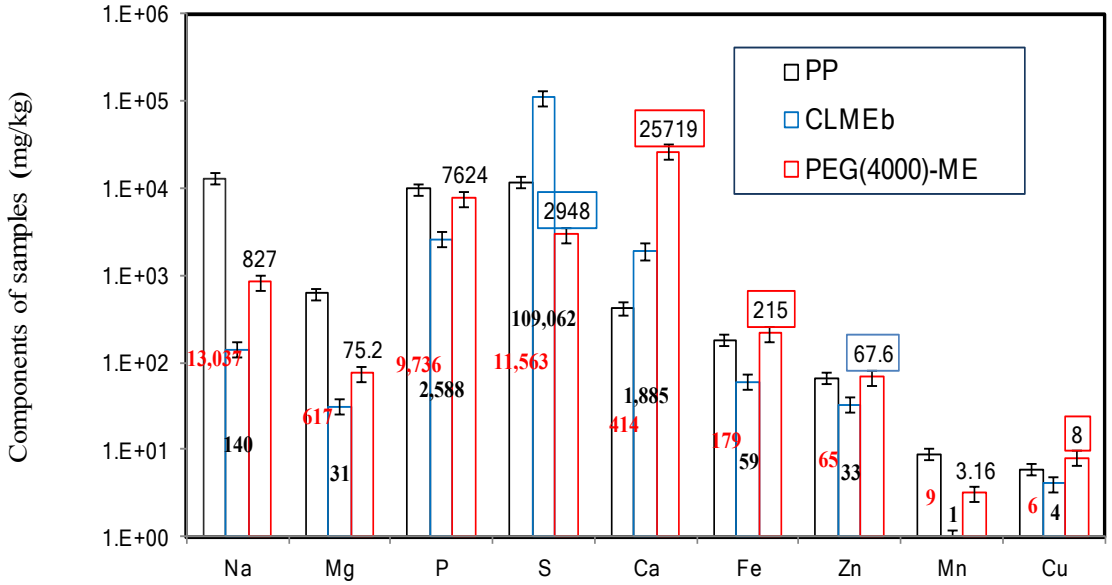

Figure S4. ICP-AES (metal) analysis results: (-□-) pea protein (PP), (-□-) $CLME_b$ (cross-linked ME treated with 30% (w/v) aqueous $(NH_4)_2SO_4$), and (-□-) PEG (4000)-ME (not treated with $(NH_4)_2SO_4$).

Table S2. ICP-AES analysis (n=1: PP, and $CLME_b$ (before FD and after FD))

	Sample	g	mL	Status	ICP								
					Na	Mg	Si	P	S	Ca	Fe	Zn	Mn
	Blank	—	—		0.15	0.00	0.17	0.00	0.03	0.00	0.00	0.00	0.01
N=1	PP	0.5012	100	Raw data (ppm)	65.49	3.09	0.58	48.80	57.99	2.48	0.90	0.33	0.05
				Actual (mg/kg)	**13037**	**617**	**81.2**	**9736**	**11563**	**495**	**179**	**65.4**	**8.91**
	CLMEb before FD	1.0033	100	Raw data (ppm)	0.85	0.24	0.31	17.48	374.99	117.63	0.35	0.11	0.04
				Actual (mg/kg)	**69.4**	**24.2**	**13.5**	**1742**	**37372**	**11725**	**34.9**	**11.3**	**3.08**
	CLMEb after FD	0.5010	100	Raw data (ppm)	0.85	0.16	0.47	12.97	95.47	9.45	0.30	0.16	0.01
				Actual (mg/kg)	**140**	**31.3**	**58.9**	**2588**	**98890**	**1885**	**59.4**	**32.8**	**1.00**

Table S3. ICP-AES analysis (n=2: PP, and $CLME_b$ (before FD-drying and after FD-drying))

	Sample	g	mL	Status	ICP								
					Na	Mg	Si	P	S	Ca	Fe	Zn	Mn
	Blank	—	—		0.15	0.00	0.32	0.00	0.15	0.00	0.01	0.00	0.00
N=2	PP	0.4999	100	Raw data (ppm)	67.98	2.87	0.95	53.58	30.12	2.50	0.89	0.34	0.03
				Actual (mg/kg)	**13568**	**573**	**125.2**	**10718**	**5995**	**500**	**176**	**68.2**	**6.39**
	CLMEb[a] before FD	1.0027	100	Raw data (ppm)	0.86	0.24	0.61	19.38	389.76	117.83	0.39	0.13	0.02
				Actual (mg/kg)	**70.9**	**23.9**	**28.7**	**1932**	**38856**	**11751**	**38.2**	**13.3**	**2.27**
	CLMEb[a]	0.5005	100	Raw data (ppm)	0.80	0.14	0.75	13.11	392.09	9.43	0.30	0.18	0.00

	after FD			Actual (mg/kg)	**129**	**28.6**	**85.8**	**2619**	**78310**	**1885**	**58.5**	**36.8**	**0.00**

[a]$CLME_b$ includes the process of "$(NH_4)_2SO_4$" precipitation.

Table S4. ICP-AES analysis (n=3: PEG (4000)-MEs and $CLME_b$)

	Sample	g	mL	Status	ICP								
					Na	Mg	Si	P	S	Ca	Fe	Zn	Mn
	Blank	–	–		0.00000	0.00000	0.18382	0.00241	0.12336	0.00000	0.00000	0.000	0.000
N=3	PEG (4000)-ME (1)[a]	0.4994	100	Raw data (ppm)	4.1305	0.37584	0.78668	38.0755	14.7225	128.443	1.0747	0.337	0.015
				Actual (mg/kg)	**827**	**75.3**	**158**	**7624**	**2948**	**25719**	**215**	**67.6**	**3.16**
	PEG (4000)-ME (2)[b]	0.0399	25	Raw data (ppm)	0.9753	0.43717	0.46021	6.2873	22.0515	1.5947	0.2682	0.138	0.009
				Actual (mg/kg)	**611**	**274**	**288**	**3939**	**13817**	**999**	**168**	**86.8**	**5.62**
	$CLME_b$[c]	0.4986	100	Raw data (ppm)	0.8374	0.22764	0.46703	23.4985	549.375	22.5460	0.2937	0.042	0.027
				Actual (mg/kg)	**168**	**45.7**	**56.8**	**4712**	**110159**	**4515**	**58.8**	**8.40**	**5.36**

[a]PEG (4000)-ME (1) does not includes the process of "$(NH_4)_2SO_4$" precipitation but centrifugation.
[b]PEG (4000)-ME (2) includes the process of "$(NH_4)_2SO_4$" for precipitation.
[c]$CLPX_b$ includes the process of "$(NH_4)_2SO_4$" precipitation.

Table S5. ICP-AES analysis of the Cu contents of PP and $CLME_b$.

Sample		n	g	mL	Status	Cu	
						ppm	average
Blank			–	–		0.00128	–
N=1	PP	1	0.5000	100	Raw data (ppm)	0.03112	5.83
					Actual (mg/kg)	5.97	
		2	0.5018	100	Raw data (ppm)	0.02981	
					Actual (mg/kg)	5.69	
	$CLME_b$	1	0.5005	100	Raw data (ppm)	0.02114	4.07
					Actual (mg/kg)	3.96	
		2	0.5016	100	Raw data (ppm)	0.02220	
					Actual (mg/kg)	4.17	

2-3-5. IC analysis

Further, the IC analysis was done by the measurements of anions of between PP, $CLME_b$, and PEG (4000)-ME. The each sample (0.5 g) was stirred in purified water (10 mL) at room temperature for overnight. This mixture was centrifuged at 15,000 rpm for 15min. The resulting supernatant (0.1 mL) was diluted to 10 ml with purified water, and measured anions by an ion chromatography (DIONEX, ICS-90).

Table S6. IC analysis for the anions/element detections

Sample	N =	**IC analysis**

		C	H	N	S
PEG (4000)-ME (1)[a]	1	45.99	8.19	6.91	1.54
	2	46.08	8.48	6.93	1.63
	average	**46.04**	**8.34**	**6.92**	**1.59**
PEG (4000)-ME (2)[b]	1	43.56	8.81	9.63	4.61
	2	43.13	8.97	9.71	4.81
	average	**43.35**	**8.89**	**9.67**	**4.71**
$CLME_b$[c]	1	26.56	7.42	16.22	11.74
	2	26.05	7.30	16.36	12.38
	average	**26.31**	**7.36**	**16.29**	**12.06**

[a]PEG (4000)-ME (1) does not includes the process of "$(NH_4)_2SO_4$" precipitation but centrifugation.
[b]PEG (4000)-ME (2) includes the process of "$(NH_4)_2SO_4$" for precipitation.
[c]$CLME_b$ includes the process of "$(NH_4)_2SO_4$" precipitation.

2-4. Result of the section 2-3.

The raw material of $(NH_4)_2SO_4$ was retained in $CLME_b$. In addition, a comparison of the PEG (4000)-ME (not treated with $(NH_4)_2SO_4$) with $CLME_b$ shows that the former contains four times the level of iron (215 mg/kg, PEG (4000)-MEs vs 59 mg/kg, $CLME_b$) suggesting that the activity of PEG (4000)-ME could be approximately four times greater than that of $CLME_b$, if an iron electron-transfer system is incorporated. These results indicate that the initial ME-redox oxidant may be more active owing to the existence of a greater proportion of incorporated Fe.

3. Optimum scale of compound modification for asymmetric redox activity of the ME.

Using CMME (20 mg) and *rac*-**1** (1.2 mM), the activity of PEG-ME (MW: 4000) was compared for different concentrations of coating to determine the optimum concentration of PEG (4000), as shown in **Figure S5**.

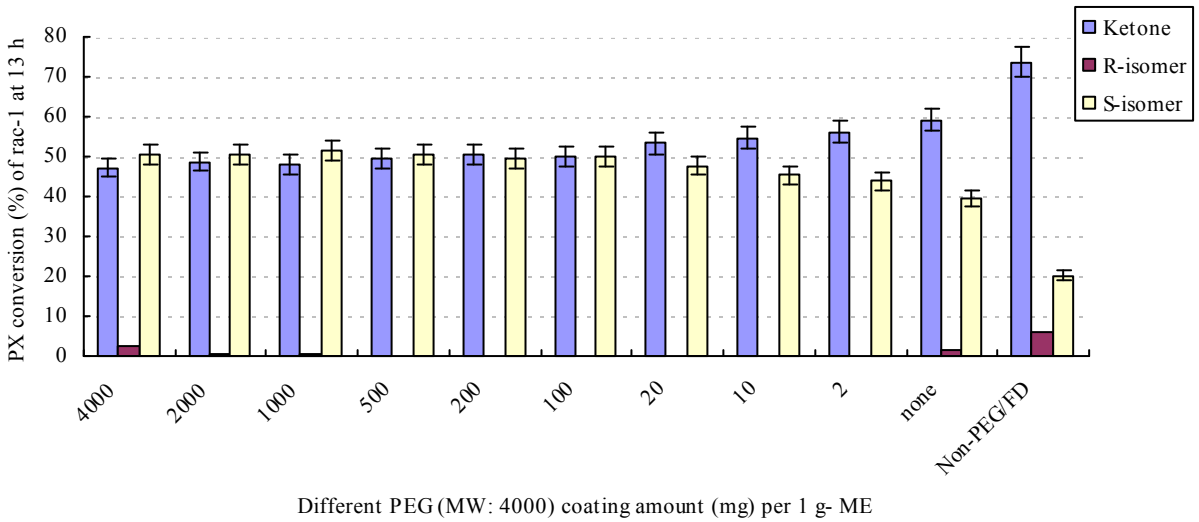

Figure S5. Conversion ratio (%) for the reaction of CMME (20 mg) with *rac*-**1** (1.2 mM) in distilled water (4.0 mL) and DMSO (0.6% (v/v)) at 40 °C with magnetic stirring at 700 rpm for 13 h: Differences in the amount of PEG (4000) coating (0–4000 mg) on the ME (1 g).

The reaction was further examined to determine whether the substrate solution (30 μL, 20,000 ppm) can be added in three portions (0 h, 8 h, and 12 h) to the CMME (20 mg) in 4.0 mL deionized water (D.W.) without any loss of optical purity or chemical yield, as shown in **Figure S6.**

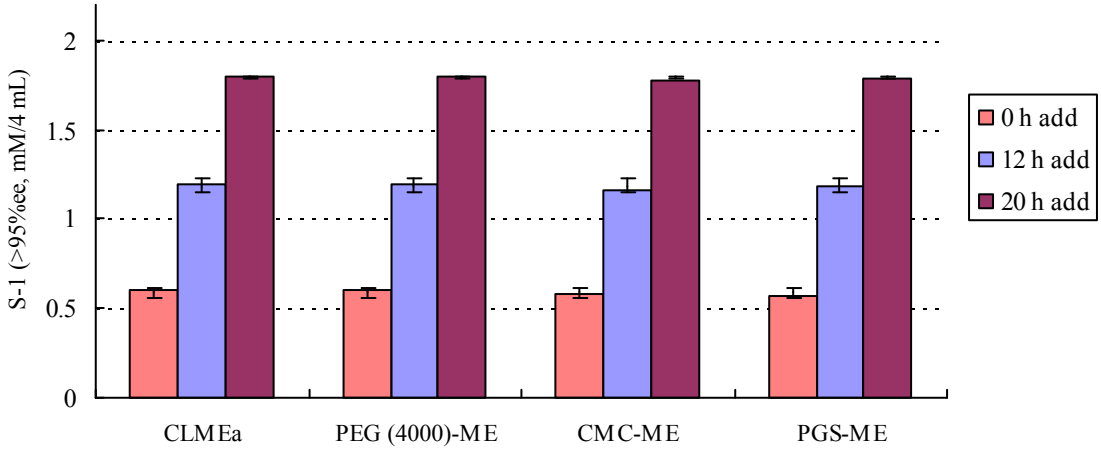

Figure S6. Conversion ratio (%) for the reaction of CMME (20 mg) with *rac*-**1** (1.2 mM) in distilled water (4.0 mL) and DMSO (0.6% (v/v)) at 40 °C with magnetic stirring at 700 rpm for 13 h: 30 h reaction of *rac*-**1** added in three portions at reaction times of 0, 12, and 20 h (1.2 mM × 3).

Scheme 1S. Microscope photographs of the ME-surfaces that are surrounded by 2.6%-Ca^{2+} or Ca^{2+}-compound

MEs-dried	AGME (PEG(MW: 4000/1000=1/2)-aggregation)		PEG (4000)-MEs
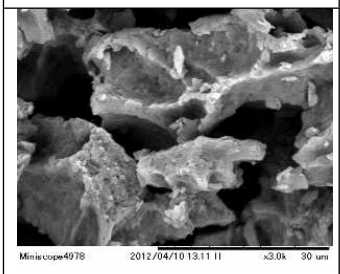	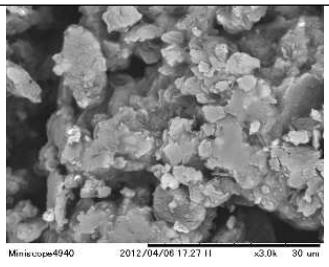	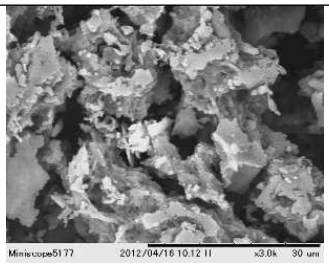	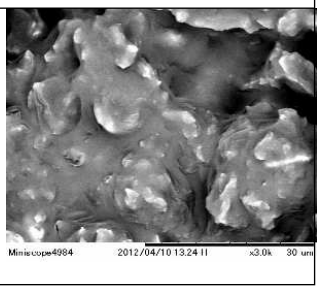

3-2. Result of the section 3-1

When an equimolecular amount of the highly polymerized compound compared to ME is used, the PEG (4000)-ME, CMC-ME, and PGS-ME (20 mg) systems only oxidize the (*R*)-isomer with high enantioselectivity at 13 h; thus, greater than 99% ee of the (*S*)-isomer was obtained from *rac*-**1**. In addition, the increase in both the product ketone and unreacted (*S*)-isomer in the aqueous medium was not lost until after three additions (30 h reaction), and the substrate could be added in three portions at 0 h, 8 h and 12 h without any decrease in optical purity or yield. Thus, using CMME (20 mg in 4.0 mL D.W.), (*S*)-**1** (approximately 1.0 mg, 99% ee) was generated from *rac*-**1** (3.6 mM) in 30 h, as shown in **Figure S6**. Furthermore, if no compound modification was applied, no stereoselectivity was observed in the reaction (i.e., non-PEG/freeze-dried (FD): no PEG (4000) and no freeze-drying) with *rac*-**1**, and both isomers were oxidized to the corresponding ketone. These results thus indicated that ME-compound modification improves the intensity and/or stereoselectivity of asymmetric oxidation in aqueous media, as shown in **Figures S5 and S6**, and implies that a ME-active site surrounded by 2.6% Ca^{2+} or Ca^{2+}-compounds may affect the ability of the reactant to enter beyond the metallic surface after GA-/highly polymerized compound treatment.

4. Data for the specific activity (unit/(mg·min)) of CMME and AGME.

This section examines the asymmetric oxidation activity of $CLME_a$ and the oxidation activity of AGME (5, 10, 15, and 20 mg) with *rac*-**1** (1.2 mM) at 40 °C under magnetic stirring at 700 rpm for 34-h bioconversions in aqueous media (4.0 mL D.W.) with water miscible DMSO (<1.0%) to determine the unit of activity.

4-1. Specific activity (unit/(mg·min))

During the 34-h incubation at 40 °C, the substrate solution (30 μL, 20,000 ppm) was added in three portions at 0, 12, and 20 h**.** Table 3-1 show the dependence of the specific activity (unit/(mg·min)) on the quantity of $CLME_a$ and AGME (mg), respectively. The unit indicates that the enzyme amount is capable of oxidizing *rac*-**1** (1 μmol) per minute. The unit indicates that the enzyme amount (mg) is capable of oxidizing *rac*-**1** (1 μmol) per minute.

Table S7. Differences in the specific activity (unit/(mg·min)) of $CLME_a$ and AGME. Details of the calculation formulas and results are noted below the table.

$CLME_a$ (mg)	Instant velocity (IV) (mM/h)	Activity (AC) (unit/(4 mL·min))	Specific activity (SA) (unit/(mg·min))
5	0.045[a]	0.003[a]	**0.0006**[a]
10	0.0675[a] 0.085[b]	0.0045[a] 0.00567[b]	0.00045[a] 0.000567[b]
15	0.068333333[a] 0.125[b]	0.004555556[a] 0.008333333[b]	0.000303704[a] 0.000555556[b]
20	0.075[a] 0.15[b]	0.005[a] 0.01[b]	0.00025[a] 0.0005[b]

AGME (mg)	Instant velocity (IV) (mM/h)	Activity (AC) (unit/(4 mL·min))	Specific activity (SA) (unit/ (mg·min))
5	0.06[c]	0.004[c]	**0.0008**[c]
10	0.098[c] 0.13[d]	0.006533[c] 0.0867[d]	0.000653[c] 0.000867[d]
15	0.12[c] 0.20[d]	0.008[c] 0.01333333[d]	0.000533[c] 0.00088[d]
20	0.15[c] 0.25[d]	0.01[c] 0.016667[d]	0.0005[c] 0.0008[d]

Calculation formula and data in CLME and AGME

IV (see Figure 5a) = Δ ketone (mM) ÷ Time (h)

AC = IV (mM/h) × 0.004 (4 mL/L) × 1000 (M/mM) ÷ 60 (min/h), SA = AC (unit/4 mL per min) ÷ $CLPC_a$ (mg)

[a]Upper shows the data of "Max IV in the 1st stage (0.6 mM: 8–12 h)"

[b]Under shows the data of "Max IV in the 2nd stage (0.6 mM– 1.2 mM: 16–18 h)"

[c]Upper shows the data of "Max IV in the 1st stage (1.2 mM: 8– 12 h)"
[d]Under shows the data of "Max IV in the 2nd stage (1.2 mM– 2.4 mM: 1– 18 h)"

4-2. Results of section 4-1.

The results indicate that the activity of $CLME_a$/AGME is approximately 0.6 mU/0.8 mU. Overall, in comparison to AGME, the unit of $CLME_a$ appears to be lower because of the particle sizes of PEG (1000 or 4000) being utilized. The solubility of *rac*-**1** (1.2 mM) is difference with PEG (MW: 4000/1000 = 1/2 or MW: 4000) in water (4 mL) containing 0.6% (v/v) DMSO: In the solubility, PEG (MW: 4000/1000 = 1/2) may be higher than PEG (4000). Thus, the ME-dried (20 h) working with a pure dehydrogenase activity for biotransformation may be surmountable in the presence of added PEG (MW: 1000/4000 = 2/1 or MW: 4000).

5. Gel-filtration for given a single band in F from many band in A (see SDS-PAGE)

The ME-suspension (10 mL) eluted from the PP-gel, which was incubated for 48 h, was first separated using a gel-filtration system. These were determined using a ÄKTA explorer 10S system. Sample (10 mL or 2 mL) was injected onto a HiLoad16/60 Superdex 200 pg column at 4 °C. Conductivity-**brown**, 280 nm-**blue**, 254 nm-**pink**, and 340 mn-**red**.

Figure S7. Gel-filtration chromatograms:

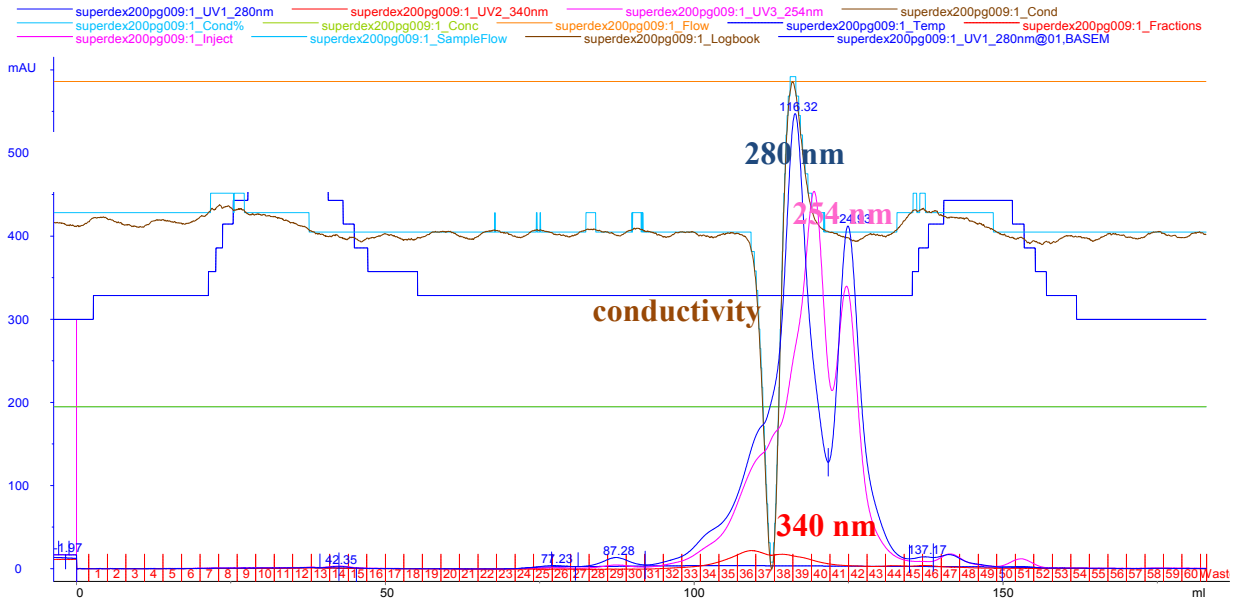

Figure S8. The supernatant of the 5% PP aqueous suspension acquired by centrifugation (2 mL).

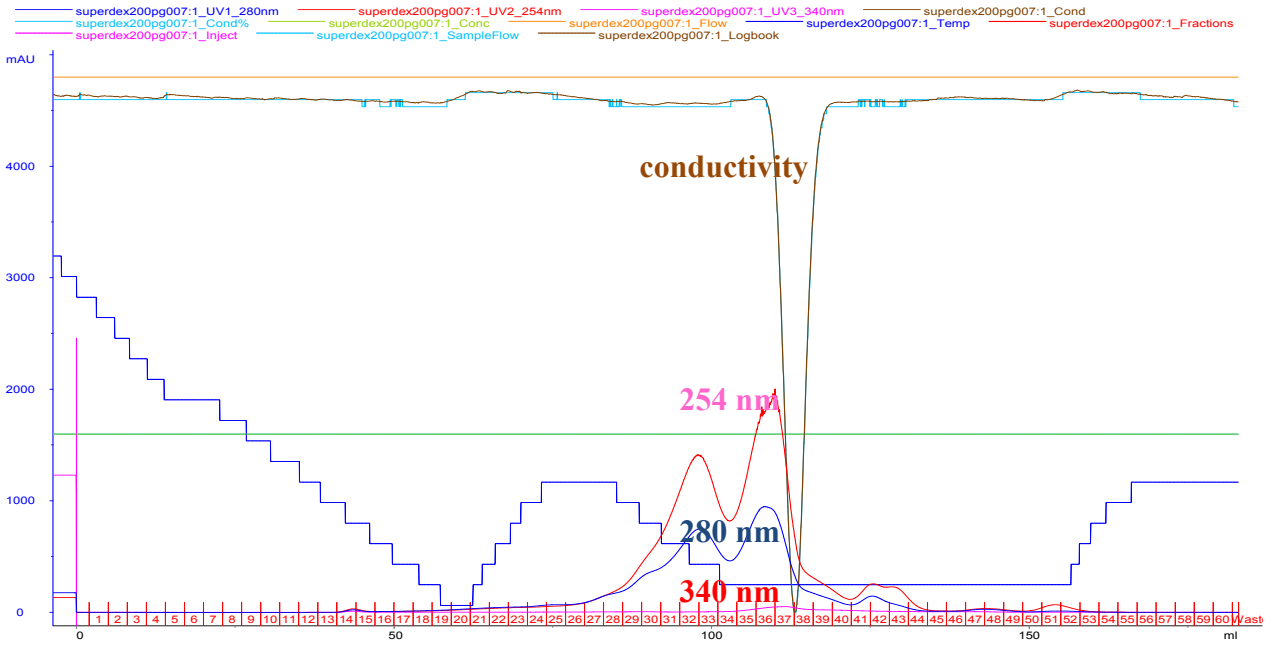

Figure S9. Data of the supernatant (2 mL) of the molecular standard: a, ferritin (440 kDa); b, aldolase (158 kDa); c, conalbumin (75 kDa); d, ovalbumin (44 kDa); e, carbonic anhydrase (29 kDa); f, ribonuclease A (13.7 kDa); g, aprotinin (6.5 kDa).

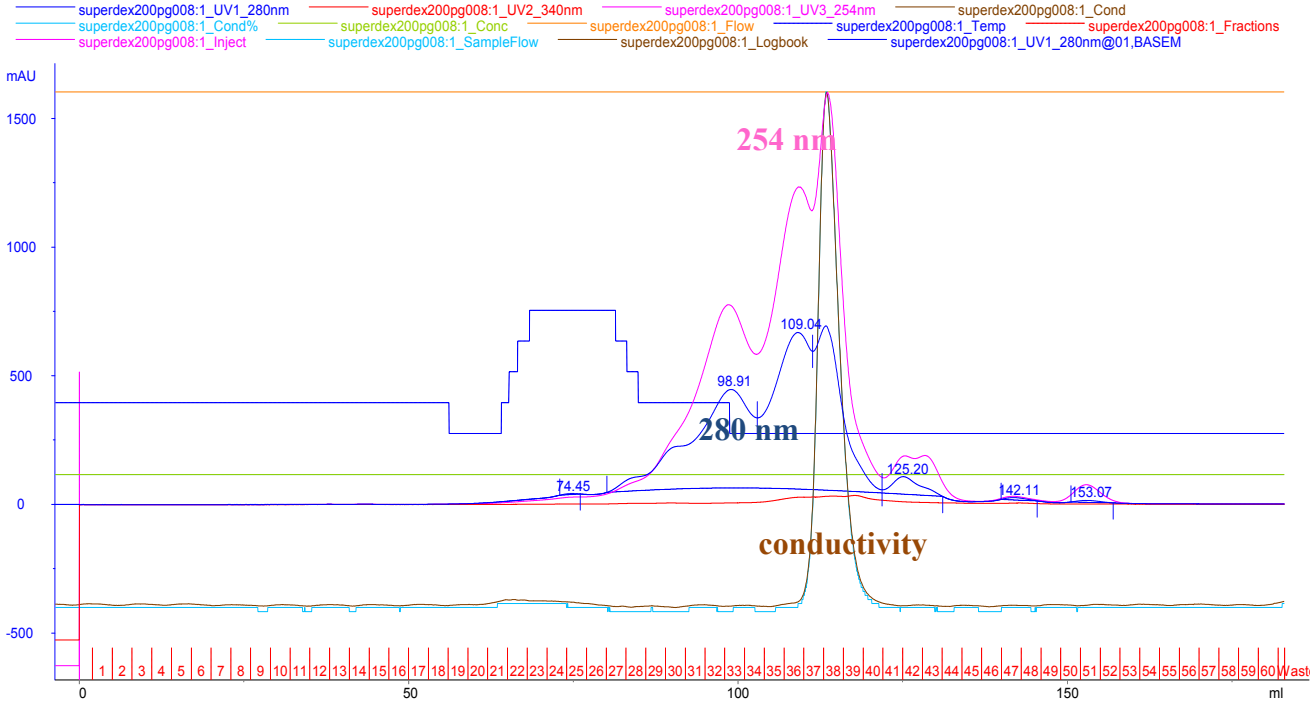

5-2. Results of the section 5-1.

As shown in **Figures S7-S9**, there are significant differences in the absorbance chromatograms of conductivity (**brown**). This is caused by the deferent conductivity between Tris-HCl (50 mM) NaCl (150 mM, pH8.0) and ME-suspension (10 mM, water). Interestingly, the suspension-injected (10 mL) can be successfully purified with sample **A** in SDS-PAGE to give a single band in **F**: the molecular mass of fraction 36 is not detected by 20 kDa but by 6.5 kDa. This means that the purpose of the gel-filtration chromatograms could be in the purification of sample **A** to sample **F**.

6. Physicochemical analysis for the detection of ME-HBP

6-1. Bradford method for the sample of SDS-PAGE

In SDS-PAGE result, the different concentrations of sample **F** (ME-redox protein), sample **A**, and sample **B** (i.e., **A** and **B** are the suspensions for producing $CLME_a$) was evaluated for the ME-redox protein concentration, and therefore, their concentrations were examined using the Bradford method

Table S8. Bradford method for the sample **F**, and the **Fs** in sample **A** and **B.**

Samples		Bradford method for protein conc. analysis			
		whole conc.(X)	F conc.(Y)	X/Y	Y/X% (v/v)
A	MEs suspension eluted from PP-gel	270 μg/mL	14.9 μg/mL	18.1	5.5%
B	Aqueous suspension of A precipitate by centrifugation	298 μg/mL	20.5 μg/mL	14.5	6.9%
F	Fraction 36 gel-filtrated from sample A	49 μg/mL	—	—	—

*In the SDS-PAGE result, Red is precipitate, Green is supernatant, DE are treated with $(NH_4)_2SO_4$).

6-1-2. PMF /LCMS-IT-TOF analysises and MASCOT analysises for six bands

Further, In-gel digestion of the other six obtained bands (single bands 1–6 monitored by SDS-Page) was optionally performed by PMF. Also, the data obtained by MASCOT analysises are shown below.

Table S9. MASCOT analysis of the band 1-6 in SDS-PAGE

Band	Score	MASCOT hit

1	77	Na^+-type flagellar protein MotY precursor
2	79	unnamed protein product [Clostridium ljungdahlii DSM 13528]
3	79	GTP diphosphokinase [Phascolarctobacterium succinatutens YIT 12067]
4	80	extracellular ligand-binding receptor [Desulfovibrio africanus str. Walvis Bay]
5	> 46	oligopeptide ABC transporter substrate-binding protein [Brevibacillus brevis NBRC 100599]
6	72	conserved hypothetical protein [Wolbachia endosymbiont of Drosophila ananassae]

6-2. Result of the section 6-1.

These result also indicated that the ratio of the ME-redox protein per MEs is approximately 1/15– 1/ 20 (~5%– 7%) (see **Table S8**), and the others (>90%) of MEs mainly contain PP's wreck from the cell membrane or cell wall, such as an extracellular ligand-binding receptor (band 4) or oligopeptide ABC transporter substrate-binding protein (band 5) (see **Table S9**).

6-3. N-terminal amino acid sequence and BLAST analysis of fraction 36 (band 7 in SDS-PAGE).

N-terminal amino acid sequence (protein sequencing) was accomplished using the protein sequencer PPSQ-21A (Shimadzu) with single band 7 of the ME-redox protein in sample F monitored by SDS-Page.

Table S10. BLAST query sequence analysis with N-terminal sequence (33 residues) identified.

Accession	Region	MW	Length	Query coverage	E value
YP 262445.1[a]	**HasAp**	**20853**	**205**	**93%**	**2e-11**
3ELL A	HasAp	NA[b]	185	93%	4e-8
YP 001347105.1	HasAp	20717	205	93%	5e-8
ZP 01366858.1	HasAp	20786	205	93%	5e-8
NP 252097.1	HasAp	20772	205	93%	5e-8
AAT49927.1	HasAp	NA[b]	206	93%	5e-8
GAA21312.1	HasAp	NA[b]	219	93%	5e-8

3MOL A	HasAp	NA [b]	184	93%	7e-6

[a]YP 262445.1: The accession hit on the query sequence was limited between the query coverage (>93%) and E value (2e-11), a 20.853 kDa HasAp gene product [*Pseudomonas fluorescens Pf-5*] from plant commensal bacteria, that can inhibit the rhizosphere and produce secondary metabolites that suppress soilborne plant pathogens.[9]
[b]NA = no BLAST correlation.

6-4. Result of the section 6-3.

Although no BLAST-hit data exemplifying an HasAp gene was detected from the plant (**Table S10**), for the connection between HBP [*Pseudomonas fluorescens Pf-5*][2] and PP, it is thought that the existence of the PP-HasAp gene (hemophore)[5] may be due to broad acquisition by the plant rather than by bacterial contamination (e.g., PP), This is indicated by the consistency of both the location of pea utilized (i.e., PP-origin: not rhizosphere but bean therein[2]) and the germfree process of MEs-purification. In addition, as direct evidence of PP-heme, it has been reported that the plant-HBP[3a] and bacterial-HBP[3b] produce secondary metabolites.[3] Thus, the PP-HBP, incorporating iron electron-transfer system in the presence of oxygen ($Fe^{2+} \rightleftarrows Fe^{3+}$ with O_2), being seen when O_2 is varied, as occurs for P450 and/or Cyt*c*O,[4a-4c] may be enabled.[4-5] In addition, the MEs-activity is competitively inhibited by the addition of a chelating agent such as 1.0 mM EDTA.[1]

7. Chromatograms of the N-terminal amino-acid sequence of band-F

Another PDF file "Protein sequence chromatogram" shows the raw data of 33 amino-acid sequence (see Table 4) detected by PPSS-21A protein sequencer (Shimazu).

8. References attached by PDF

(1) H. Nagaoka, K. Udagawa, K. Kirimura, *Biotechnol. Prog.* **2012**, *28*, 953–961.

(2) I. T. Paulsen, C. M. Press, J. Ravel, D. Y. Kobayashi, G. S. Myers, D. V. Mavrodi, R. T. DeBoy, R. Seshadri, Q. Ren, R. Madupu, R. J. Dodson, A. S.

Durkin, L. M. Brinkac, S. C. Daugherty, S. A. Sullivan, M. J. Rosovitz, M. L. Gwinn, L. Zhou, D. J. Schneider, S. W. Cartinhour, W. C. Nelson, J. Weidman, K. Watkins, K. Tran, H. Khouri, E. A. Pierson, L. S Pierson 3rd, L. S. Thomashow, J. E. Loper, *Nat. Biotechnol.* 2005, **23(7)**, 873.

(3) (a) W. Adam, W. Boland, J. Hartmann-Schreier, H-U. Hump, M. Lazarus, A. Saffert, C. R. Saha-Moller, P. Schreier, *J. Am. Chem. Soc.* 1998, **120,** 11044. (b) M. Landwehr, L. Hochrein, R. C. Otey, A. Kasrayan, E. J. Bäckvall, H. F. Amold, *J. Am. Chem. Soc.* 2006, **128,** 6058. (c) A. R. McDonald, M. R. Bukowski, E. R. Farquhar, T. A. Jackson, K. D. Koehntop, Mi Sook Seo, R. F. De Hont, A. Stubna, J. A. Halfen, E. Muonck, W. Nam, L. Que Jr. *J. Am. Chem. Soc.* 2010, **132**, 17118.

(4) (a) D. S. Lee, H. Yamada, H. Sugimoto, I. Matsunaga, H. Ogura, K. Ichihara, S. Adachi, S. Y. Park, Y. Shiro, *J. Biol. Chem.* 2003, **278,** 9761. (b) O. Shoji, T. Fujishiro, H. Nakajima, M. Kim, S. Nagano, Y. Shiro, Y. Watanabe, *Angew. Chem. Int. Ed*. 2007, **46,** 3656. (c) T. H. Yosca, J. Rittle, C. M. Krest, E. L. Onderko, A.-R. K. Beham, M. T. Green, *Science* 2013, **342,** 825. (d) P. R. Ortiz de Montellano, *Cytochrome P450*: *Structure, Mechanism, and Biochemistry*, 3rd ed.; Kluwer Academic/Plenum: New York, Boston, Dorcrecht, London, Mosow, 2004.

(5) (a) M. L. Oldham, D. Khare, F. A. Quiocho, A. L. Davidson, J. Chen, *Nature* 2007, **450,** 515. (b) S. Krieg, F. Huché, K. Diederichs, N. Izadi-Pruneyre, A. Lecroisey, C. Wandersman, P. Delepelaire, W. Welte, *PNAS* 2009, **106(4)**, 1045. (c) N. Izadi-Pruneyre, N. Wolff, V. Redeker, C. Wandersman, M. Delepierre, A. Lecroisey, *J. Bacteriol.* 1999, **261,** 562. (d) S. Létoffé, K. Omori, C. Wandersman, *J. Bacteriol.* 2000, **182 (16),** 4401.